PERFORMANCE AND TOLERANCE STUDIES OF THE X-RAY PRODUCTION FOR THE X-BAND FEL COLLABORATION

J. Pfingstner*, E. Adli, University of Oslo, Oslo, Norway

Abstract

The X-band FEL collaboration is currently designing an X-ray free-electron laser based on X-band acceleration technology. This paper reports on the recent progress on the design of the undulator part of this machine including simulations of the X-ray production process. The basic parameters have been chosen and a beam transport system has been designed, considering strong and weak focusing of quadrupole and undulator magnets. Simulations of the X-ray production process have been carried out with realistic input beam distributions from particle tracking studies of the linac design team. The expectable X-ray properties for SASE and seeded FEL operation have been investigated and also undulator taper options have been studied.

INTRODUCTION

The X-band collaboration is a group of 12 institutes and universities with the common interest of using X-band acceleration technology for FEL applications. The higher acceleration gradients achievable with X-band structures allow making linacs shorter and more power efficient as S-band and C-band linac used nowadays. The recent advances in the X-band technology [1] have encouraged the X-band collaboration to design a soft and a hard XFEL based on the X-band technology [2]. An important part of this effort is the design of the undulator section and the simulation of the X-rays production process, which is the subject of this paper. Topics that will be covered are the basic parameter choice, the beam transport lattice, and the simulations of the most important X-ray parameters for different modes of operation.

UNDULATORS AND ELECTRON BEAM

The parameter of the electron beam and the undulator section are chosen by taking into account the experience of existing facilities, e.g. SwissFEL [3] and LCLS [4]. The undulator section consists of 13 permanent magnet undulators [5] of each 3.96 m in length. The undulator magnets have a period length λ_u of 15 mm and a maximal undulator parameter K of 1.3, which allows reaching an X-rays wavelength of 1 Å with a beam energy of 6 GeV. The modules are separated by gaps of 0.72 m to provide space for quadrupole magnets, beam position monitors, beam loss monitors and phase shifters. The quadrupole magnets are used to control the beam size (FODO lattice) as will be discussed below.

With the described undulator parameters, a beam energy of about 6 GeV is necessary to reach the specified X-ray wavelength of 1 Å. The beam current has to be >3 kA to enable the production of X-ray with on a GW level, and to achieve a reasonably short saturation length. Preferably the beam current should be uniform along the bunch, which implies a bunch charge of 200 pC assuming a bunch length of about 15 μm. To keep the electrons and the X-rays in a resonance condition, there are limits on the transverse emittance ϵ and the energy spread σ_E of the electron beam [6], which are for the chosen parameters <0.3 μm and <2x10^{-4}, respectively.

An electron beam B0 with the stated properties has been created artificially and will act in the performed simulations as a reference. Complementary, two beams, B1 and B5, have been provided by the linac team, which have been created with particle tracking using PLACET [7]. In contract to B0, the bunch charge of B1 and B5 is 250 pC. The two beams correspond to different bunch compressor setups. As can be seen in Fig. 1, neither B1 nor B5 reach the specified beam current yet, since the optimisation of the linac and the bunch compressors is an on-going effort.

BEAM TRANSPORT SYSTEM

The electron beam size is controlled in the undulator section due to the focusing of the quadrupole magnets, which are located in the gap between the undulator magnets. The magnet strengths are adjusted to form a FODO lattice. The size of the β-function is a trade off between high current density (small β-function), and small longitudinal velocity change of the electrons due to their betatron motion (large β-function). An expression for the optimal average β-function β_{opt} has been derived in [8] and is for our parameters 15 m.

If only the strong focusing of the quadrupole magnets is considered, the lattice design can be performed with simple

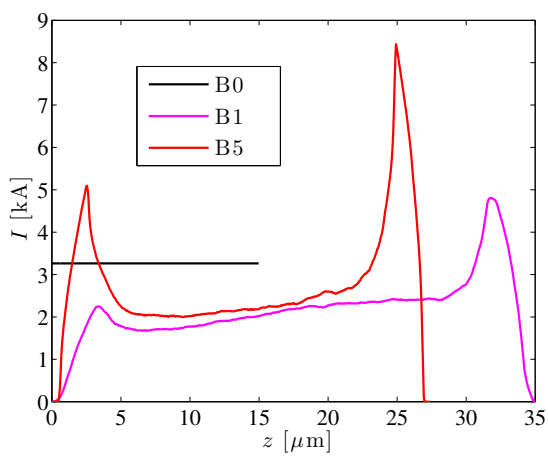

Figure 1: Current profile along the different considered bunches. B0 is an artificially created reference bunch.

* juergen.pfingstner@cern.ch

ISBN 978-3-95450-134-2

analytic expressions. However, also the weak focusing of the magnets in vertical direction (due to the pole fringe fields) has to be taken into account. For this reason, a generalised FODO lattice is used, where different magnet strengths K_1 and K_2 for the focusing and defocusing quadrupole magnets can be chosen. This additional degree of freedom allows compensating the distortion of the β-function due to the weak focusing, and a periodic solution can be found.

To find such magnet strengths K_1 and K_2 the following optimisation problem was implemented in OCTAVE [9]

$$\min_{K_1,K_2} J(K_1,K_2), \tag{1}$$

where the target function J represents the quadratic error of horizontal and vertical β-functions for the magnet strengths K_1 and K_2 from β_{opt}

$$J(K_1,K_2) = \sum_{i\in\{x,y\}} \left(\frac{\sqrt{\beta_{i,1}} + \sqrt{\beta_{i,2}}}{2} - \sqrt{\beta_{opt}} \right)^2 .$$

The β-functions at the centres of the focusing and defocusing magnets $\beta_{x,1}$, $\beta_{x,2}$, $\beta_{y,1}$ and $\beta_{y,2}$ are calculated from the according beam transport matrices M as [10]

$$\beta_{x,1} = \frac{M_{x,1}(1,2)}{\sin(\mu_{x,1})} \quad \text{with}$$
$$\mu_{x,1} = \text{acos}\left(\frac{\text{trace}\,(M_{x,1})}{2} \right).$$

In this case $M_{x,1}$ is the horizontal beam transport matrix for one FODO period starting from the centre of the quadrupole magnet with strength K_1. The matrices M are computed by the multiplication of the transport matrices of the individual elements. While an undulator magnet is modelled as a simple drift space in the horizontal direction, the vertical transport matrix is given by

$$M_{y,U} = \left(M_{y,P/2} \right)^{2N_P},$$

where N_p is the number of undulator periods of length λ_u, and $M_{y,P/2}$ is the transport matrix of one undulator pole given by

$$M_{y,P/2} = \begin{bmatrix} 1 & 0 \\ -\frac{1}{f_f} & 1 \end{bmatrix} \begin{bmatrix} 1 & \lambda_u/2 \\ 0 & 1 \end{bmatrix} \begin{bmatrix} 1 & 0 \\ -\frac{1}{f_f} & 1 \end{bmatrix}. \tag{2}$$

Eq. 2 represents fringe field kicks at the entrance and the exit of a magnet pole and a drift space in between the poles. The kick strength $1/f_f$ of the vertical fringe fields is given by [10]

$$\frac{1}{f_f} = \frac{\pi^2 K^2}{2\gamma^2 \lambda_u},$$

where γ is the relativistic factor of the electron beam. The OCTAVE optimisation routine `fminsearch` was used successfully to find a solution to the optimisation problem Eq. 1. In tracking simulations with GENESIS [11], it has been verified that the corresponding β-functions are regular and of the desired size β_{opt} in both transverse dimensions.

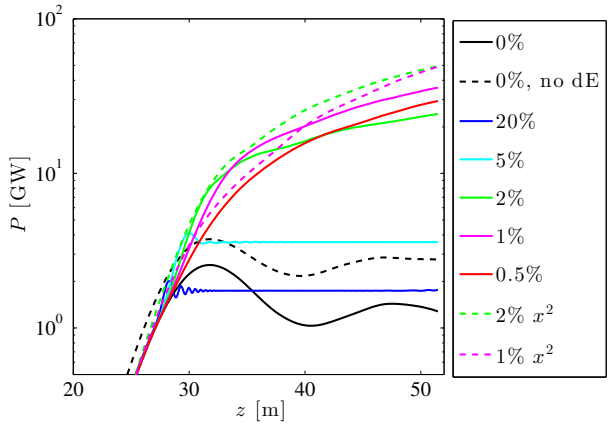

Figure 2: X-ray power along the undulator section for different undulator taper types. The percentage mentioned in the label corresponds to the decrease of the undulator parameter K at the end of the undulator section.

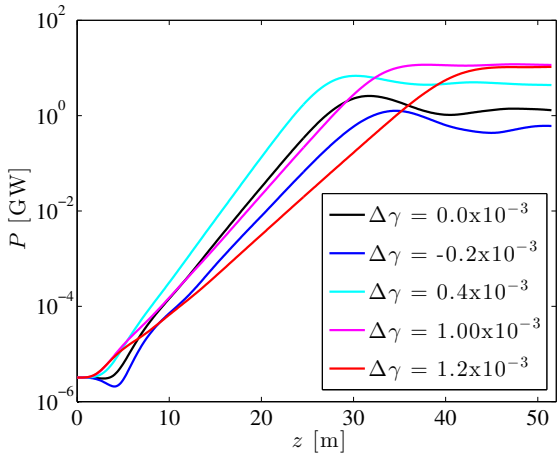

Figure 3: X-ray power along the undulator section for seeded operation with different beam energy detuning $\Delta\gamma$.

SIMULATION STUDIES

The studies of the X-ray production process are mainly carried out with the help of simulation with the FEL code GENESIS [11]. The plausibility of the results is checked with analytical estimates known from FEL theory, e.g. [6]. In the following, the performed simulations will be grouped according to the used simulation mode. Single micro-bunch simulations can be performed very rapidly and are a good approximation for the operation with a strong seed laser. Even though single micro-bunch simulations can be used to study many effects, computationally much more expensive multiple micro-bunch simulations are necessary to be able to take into account all properties of the used electron beam. This is in particular necessary to study the SASE process.

Before the study of the X-ray production process started, suitable simulation parameters were determined. In systematic studies it was found that a particle number per slice of 2^{13} was sufficient. Also it was found that space charge

ISBN 978-3-95450-134-2

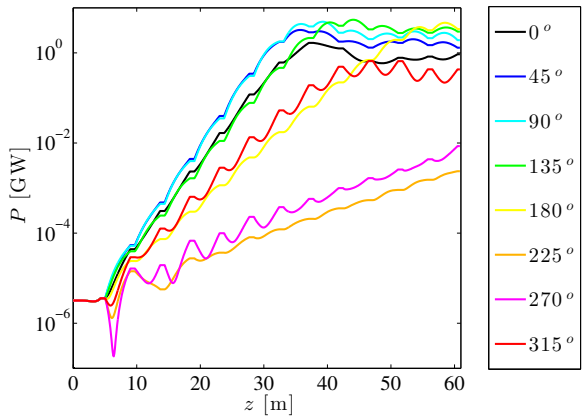

Figure 4: X-ray power along the undulator section for different phase mismatches between electron and X-ray beam introduced in the gaps between the undulator magnets.

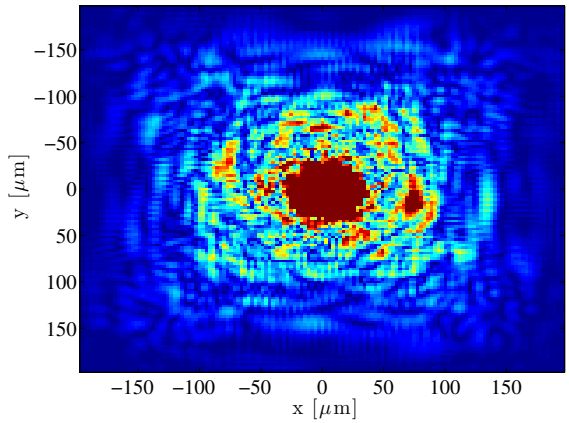

Figure 5: Transverse X-ray intensity at the end of the undulator section created with beam B0 in seeded operation.

effects have a negligible effect on the X-ray production, due to the high energy of the electron beam. Hence, the time-consuming space charge calculation was turned of in the GENESIS simulations. Also the effect of incoherent synchrotron radiation was investigated. While the corresponding beam energy spread increase can be neglected, the average association beam energy loss has a rather strong impact on the simulation results and has to be taken into account, as can be seen from the solid and dashed black lines in Fig. 2.

Single Micro-Bunch Simulations

The produced X-ray power for a seeded operation is around 1–2 GW with an saturation length of 32 m, as can be seen in Fig. 2 (solid black line). Since in this particular simulation the gaps have not been considered, the saturation length including gaps is about 37 m, which has been confirmed with simulations including the gaps.

To increase the X-ray power further, undulator strength tapering can be applied [12]. The effect of linear and quadratic tapers has been evaluated and the results are shown in Fig. 2. The tapering starts to decrease the undulator parameter K at 27 m up to a maximal percentage at the end of the undulator section. With a quadratic taper of 1–2%, the X-ray power can be increased to 52 GW. From these results it is also clear that tapering is not only compensating the beam energy loss by restoring the undulator resonance condition. This would only result in an X-ray production corresponding to the dashed black line, where the energy loss has been turned of artificially in the simulation. Instead, tapering is keeping the electrons at a relative phase with respect to the X-rays such that they continuously lose energy in the saturation regime, instead of performing synchrotron oscillations. A similar effect can be achieved in seeded operation, if the beam energy is chosen slightly higher than given by the resonance condition. With an energy detuning of 1 per mil, the X-ray power can be increase to 10 GW, as can be seen in Fig. 3.

In Fig. 4, the effect of a phase mismatch of the electron beam and the X-rays due to a wrong length of the undulator gaps has been investigated. The black curve shows the X-ray power when the resonance condition is perfectly maintained. Interestingly, for a large range of phase shifts the output power is increased, since the electrons are moved to a relative phase with respect to the X-rays where they lose more energy as for the nominal condition. This suggests that phase shifters could be used as an alternative to tapering to increase the X-ray power. The simulation results also indicate that the necessary phase shifter resolution should be in the order of 10-20°, which is consistent with phase shifter designs from existing facilities.

In Fig. 5, the intensity distribution of the X-rays (no tapering) at the end of the undulator section is shown. The plot is saturated in the centre where the highest X-ray power is located. This high intensity area is at the same location as the electron beam and both have about the same size. The corresponding X-rays have been created shortly before the end of the undulator (near field radiation). The radiation further away from the electron beam is of lower intensity. It has been produced further upstream in the undulator section and has diffracted to larger distances from the centre (far field radiation).

Multiple Micro-Bunch Simulations

Simulations with multiple micro-bunches are computational expensive. For the beams B0, B1 and B5, a total number of 6393, 14625 and 11433 micro-bunches have been simulated, respectively. This corresponds to a simulation of each 24th micro-bunch of the real beam, which is sufficient according to the suggested parameter choice of GENESIS. The simulations have been performed on a 32-core computer with the MPI parallelised version of GENESIS. One simulation takes about 2 1/2 hours with this setup.

The average power of the X-ray pulse along the undulator section for different beam distributions is depicted in Fig. 6. For the seeded operation, a seeding laser power of 10 kW

ISBN 978-3-95450-134-2

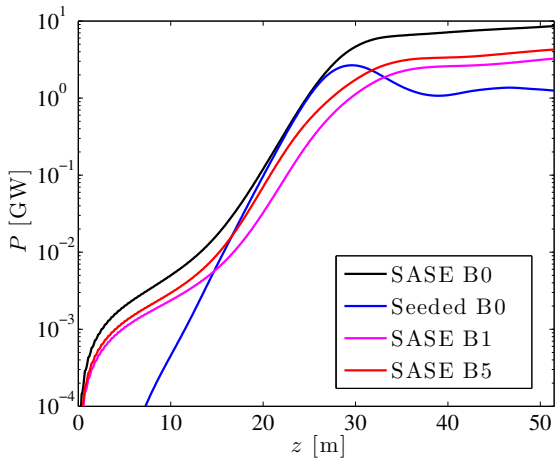

Figure 6: Average power of the X-ray pulse plotted along the undulator section. Different electron beams are considered in SASE and seeded mode.

was used, and the shot noise of the electron beam was artificially turned off. The simulations show, that the beam B0 produces 9 GW of X-ray power in the SASE mode, which is significantly more than the corresponding 1–2 GW produced in seeded operation.

Also the performance of the beam distributions created from tracking simulations with an realistic lattice setup has been evaluated. Both beams, B1 and B5, cannot reach the same X-ray power level as the benchmark beam B0. As a reason for the worse performance, the lower peak current of these beams has been identified (see Fig. 1). The currently produced beams will have to be shortened in the future to reach the necessary 3 kA. Even though B5 is shorter than B1, the produced X-ray power is hardly increased compared to B1. This is due to the fact that the current is only larger at spikes at the head and the tail of the bunch, where also the energy spread is increased, which inhibits the X-ray production process. This outcome is a valuable input for the linac and bunch compressor team as a guideline for their design.

CONCLUSIONS

The design of the undulator section and the simulations of the X-ray production process for the hard X-ray FEL of the X-band collaboration have been described. For the chosen parameters, the expectable X-ray power level is 1–2 GW and 9 GW for SASE and seeded operation, respectively. The saturation length of the FEL process is about 37 m including the gaps between undulator magnets and the expectable spectral bandwidth is 1 per mil at the end of the undulator section. Also advanced methods to increase the X-ray output power have been studied, such as tapering, detuning and a phase shifting with phase shifter magnets. For a quadratic taper of 1–2% the X-ray power can be increase to 52 GW.

In collaboration with the linac and bunch compressor team, different realistic electron beam distributions have been studied with respect to the X-ray power produced by them. This effort has resulted in design guidelines that will help to improve the overall performance of the proposed XFEL facility. In the future, it is planned to perform tolerance studies and investigate the influence of resistive wall wakefields on the X-ray production. Also, the undulator magnet parameter will be re-evaluated with the intention to minimise the cost of the overall XFEL facility.

REFERENCES

[1] A. Degiovanni et al., *High-gradient test results from a CLIC prototype accelerating structure: TD26CC*, In Proc. of IPAC14, WEPME015 (2014).

[2] J. Pfingstner et al., *The X-band FEL collaboration*, In Proc. of FEL15, TUP013 (2015).

[3] SwissFEL CDR, *SwissFEL Conceptual Design Report*, PSI Bericht Nr. 10-04 (2012).

[4] LCLS CDR, *Linac Coherent Light Source (LCLS) Conceptual Design Report*, SLAC-R-593 (2002).

[5] J. A. Clarke, *The Science and Technology of Undulators and Wigglers*, Oxford University Press 2004, ISBN 978-0-19-850855-7.

[6] P. Schmüser et al., *Free-Electron Lasers in the Ultraviolet and X-Ray Regime*, Springer International Publishing Switzerland 2014, ISBN 978-3-319-04080-6.

[7] D. Schulte et al., *The PLACET Tracking Code*, `http://clicsw.web.cern.ch/clicsw/`.

[8] E. L. Saldin et al., *Design Formulas for VUV and X-Ray FELs*, In Proc. of FEL04, MOPOS15 (2004).

[9] J. W. Eaton. Octave. `www.gnu.org/software/octave`.

[10] H. Wiedemann, *Particle Accelerator Physics*, Springer-Verlag Berlin Heidelberg 2007, ISBN: 978-3-540-49043-2.

[11] S. Reiche, *GENESIS 1.3*, `http://genesis.web.psi.ch/`.

[12] D. Ratner et al., *FEL gain length and taper measurements at LCLS*, In Proc. of FEL09, THOA03 (2009).

ISBN 978-3-95450-134-2